1 Complete Genome Sequence of the Frog Pathogen Mycobacterium

2 ulcerans ecovar Liflandii

- 3
- 4 Nicholas J. Tobias^{1,2}, Kenneth D. Doig¹, Marnix H. Medema^{3,4}, Honglei Chen⁵, Volker Haring⁵,
 5 Robert Moore^{5,6}, Torsten Seemann⁷ and Timothy P. Stinear^{1#}
- 6

7

- ¹Department of Microbiology and Immunology, University of Melbourne, Parkville, Victoria, Australia
- 8 ²Department of Microbiology, Monash University, Clayton, Victoria, Australia
- 9 ³Groningen Bioinformatics Centre, Groningen Biomolecular Sciences and Biotechnology Institute,
- 10 University of Groningen, Groningen, The Netherlands
- ⁴Department of Microbial Physiology, Groningen Biomolecular Sciences and Biotechnology Institute,
- 12 University of Groningen, Groningen, The Netherlands
- ⁵Australian Animal Health Laboratories, CSIRO, Geelong, Australia
- 14 ⁶ARC Centre of Excellence in Structural and Functional Microbial Genomics, Australia
- 15 ⁷Victorian Bioinformatics Consortium, Monash University, Clayton, Victoria, Australia
- 16
- 17 Running Title: Complete Genome sequence of Mycobacterium Liflandii
- 18
- 19 [#]Corresponding author: tstinear@unimelb.edu.au
- 20
- 21
- 22

23 Abstract

24 In 2004, a previously undiscovered mycobacterium resembling Mycobacterium ulcerans (the agent of Buruli ulcer) was reported in an outbreak of a lethal mycobacteriosis in a laboratory colony of the 25 African clawed-frog Xenopus tropicalis. This mycobacterium makes mycolactone and is one of several 26 27 strains of *M. ulcerans*-like mycolactone-producing mycobacteria recovered from ectotherms around the 28 world. Here we describe the complete 6,399,543 bp genome of this frog pathogen (previously 29 unofficially named Mycobacterium 'liflandii') and we show that it has undergone an intermediate degree of reductive evolution, between M. ulcerans Agy99 and the fish pathogen Mycobacterium 30 31 marinum M. Like M. ulcerans Agy99, it has the pMUM mycolactone plasmid, over 200 chromosomal 32 copies of the insertion sequence IS2404 and a high proportion of pseudogenes. However, M. 'liflandii' 33 has a larger genome that is closer in length, sequence and architecture to M. marinum M than to 34 M. ulcerans Agy99, suggesting that M. ulcerans Agy99 has undergone accelerated evolution. Scrutiny 35 of genes specifically lost suggests *M. 'liflandii'* is a tryptophan, tyrosine and phenylalanine auxotroph. 36 A once extensive *M. marinum*-like secondary metabolome has also been diminished through reductive 37 evolution. Our analysis shows that M. 'liflandii', like M. ulcerans Agy99, has the characteristics of a 38 niche-adapted mycobacterium but with several distinctive features in important metabolic pathways 39 that suggests it is responding to different environmental pressures, supporting earlier proposals that it 40 could be considered an *M. ulcerans* ecotype, hence the name *M. ulcerans* ecovar Liflandii.

41

<u>JB Accepts published online ahead of print</u>

42 Introduction

43 An interesting member of the Mycobacterium marinum and Mycobacterium ulcerans complex (MuMC) was discovered in the summer of 2001 when an outbreak of generalized cutaneous lesions 44 45 developed in a colony of *Xenopus tropicalis* at the University of Berkeley, California (1). Infected 46 frogs developed granulomatous skin lesions, with coelomic distention, generalised oedema and 47 septicaemia (1). Cytological examination confirmed the presence of acid-fast bacilli in smears from the 48 liver, spleen, kidney and skin. Based on histopathology and some molecular testing, it was concluded 49 that these frogs were suffering from a mycobacteriosis caused by a Mycobacterium ulcerans-like 50 bacterium (1). There are on-going reports and high lethality of this disease in captive frogs across the 51 United States (US) and those imported from the US to Europe (2-4), but this mycobacterium has not 52 been reported to cause illness in humans. Further characterisation of the frog pathogen revealed that it 53 harboured М. pMUM the ulcerans megaplasmid and produced mycolactone E, a unique structural variant of the polyketide toxin that is key for pathogenesis in M. 54 55 *ulcerans* (5, 6). Limited genotype analysis suggests that a single clone of this pathogen is circulating worldwide in institutions housing and breeding anurans. The species name Mycobacterium liflandii 56 57 was proposed, although as the authors admitted at that time, the data were lacking to conclude that this 58 mycobacterium constituted a separate species (6).

59

<u>JB Accepts published online ahead of prini</u>

A recent genomic study of 35 MuMC isolates confirmed earlier indications that all mycolactoneproducing mycobacteria, including those strains classically considered *M. ulcerans*, evolved by a process of lateral gene transfer and reductive evolution from a common *M. marinum*-like progenitor (7-9). These comparisons also show at least three discrete, deep-branching lineages of mycolactone producers, which include the strains predominantly infecting ectotherms and those strains commonly causing Buruli ulcer in humans (7-9). All lineages showed evidence of strong selective pressures acting on the same cell wall-associated genes, but the lineages differed in the extent of genome reduction, suggesting each lineage might be adapting to slightly different niche environments (8). The frog pathogen belongs to lineage 1, while *M. ulcerans* isolates from Africa and Australia belong to lineage 3. Hereafter we will refer to this frog pathogen as *M. ulcerans* Liflandii (abbreviated as *Mu*L) in line with our proposition that *Mu*L and other lineage-specific isolates should be considered ecotypes of *M. ulcerans* (8, 10).

72

Like other MuMC members, *MuL* grows preferentially around 32°C. However, it exhibits several distinguishing microbiological characteristics. *MuL* forms rough, light orange, non-photochromogenic colonies on Middlebrook 7H11 agar supplemented with oleic acid, albumin, dextrose and catalase (37, 56). *MuL* grows better on charcoal medium than Lowenstein-Jensen (LJ) medium whereas classical (lineage 3) *M. ulcerans* isolates do not grow on charcoal. Like *M. ulcerans*, antibiograms of *MuL* indicate resistance to isoniazid, ethambutol and ethionamide but *MuL* is reportedly additionally resistant to rifampicin and clarythromycin (53).

80

To date the MuMC are represented by only two fully assembled genome sequences; an *M. ulcerans* isolate from a Buruli ulcer patient isolated in Ghana in 1999 and a *M. marinum* clinical isolate obtained from a patient in the United States in 1994 (11, 12). The high complexity of *M. ulcerans* genomes with the repeat-rich nature of the mycolactone polyketide synthase genes (harboured on pMUM plasmid) and >200 chromosomal copies of IS2404 has been a barrier to completing assemblies of genome sequences from other members of this complex. Here we describe and compare the sequenced and fully assembled chromosome of *Mu*L, which together with our previous description of the pMUM002 89 increasingly associated with epizoonotics in fish, frogs and other ectotherms around the world.

90

<u>JB Accepts published online ahead of print</u>

91 Materials and Methods

92 Strain and culture conditions

93 M. ulcerans Liflandii 128FXT was originally isolated from infected Xenopus tropicalis at the 94 University of California, Berkeley (1). The isolate was cultured on Brown and Buckle egg yolk agar 95 slopes at 30°C. Rifampicin MIC testing was performed using Mycobacterial Growth Indicator Tubes 96 (MGIT) as described (13). Briefly, MuL at a McFarland standard of 0.5 was prepared as recommended 97 by the manufacturer (Becton Dickinson) and diluted 1:5 in sterile saline. MGITs were enhanced with 98 800 µl of MGIT SIRE supplement (Becton Dickinson) and inoculated with 0.5 ml of the diluted 99 bacterial suspension. MGITs contained two-fold dilutions of rifampicin from 0.0625 µg/ml to 16 100 µg/ml. Experiments were established in triplicate for each dilution. MGITs were incubated at 30°C and 101 examined daily for four weeks at a wavelength of 365nm, noting the time to fluorescence.

102 DNA Methods

Genomic DNA was extracted from *MuL* as previously described (9). Standard methods were used for
PCR and Sanger sequencing.

105 Whole Genome Sequencing and Assembly

Roche 454 GS-FLX sequencing was employed to obtain 260,654 single-end reads (106.3 Mbp) and
 assembled using gsAssembler v2.5.3 into 91 scaffolds containing a total of 622 contigs. Scaffolds were
 ordered by reference to an optical map (see below) and BLAT searches in Projector 2 against the *M*.

109 marinum M and M. ulcerans Agy99 reference genomes (14). Genome finishing was managed with 110 Gap4 (15). Specific oligonucleotides were designed to contig-flanking sequences and PCR with Sanger 111 sequencing was used to close gaps. Wherever it was established that a gap contained a single copy of 112 IS2404, the gap was filled with a copy of IS2404 from the previously sequenced M. ulcerans Agy99. It is important to note therefore that the exact sequence of each copy of IS2404 in MuL has not been 113 114 established. A 3 kbp Roche 454 GS-FLX mate-pair library was also constructed and yielded 218,423 115 reads (63.6 Mbp). Finally, 13,778,118 Illumina paired-end sequencing reads (487.61Mbp) obtained from a previous project (8) were mapped to the final assembly using an in-house Python utility called 116 117 Nesoni (http://vicbioinformatics.com; Harrison et al., in preparation) with SHRiMP 2.2 (51). Nesoni 118 was used to do a global variant analysis and generate a list of differences and correct 454 sequencing 119 errors. The chromosome sequence of MuL 128FXT was submitted to Genbank under BioProject 120 number PRNJA128960.

121 Optical Mapping

An NheI optical map of *MuL* was prepared by OpGen (Wisconsin, USA) to guide assembly. Contigs
were aligned to the optical map using MapSolver software (v3.2.0).

124 Annotation and Comparative Genome Analysis

125 Genome annotation was performed by Prokka (http://vicbioinformatics.com/; Seemann, in preparation), 126 utilising the previously annotated *M. marinum* M and *M. ulcerans* Agy99 genomes as references (11, 127 12). Manual curation of the annotation was then performed using Wasabi, a web-based annotation 128 editor and database as described previously (11). Regions of difference (RDs) were identified by mapping M. ulcerans Agy99 and M. marinum de novo contigs to the assembled MuL genome. This 129 130 mapping and other comparisons were visualized with Circos (16), Mauve (17) and ACT (18). 131 Secondary metabolite biosynthesis gene clusters were identified using antiSMASH (19). Additional 132 pseudogene clusters that were too degraded for detection by antiSMASH were identified by MultiGeneBlast (<u>http://multigeneblast.sourceforge.net/</u>; Medema *et al.*, in preparation). The final, manually determined, cut-off used to define gene cluster orthology was that gene clusters should have at least 40% genes with at least 60% amino acid sequence identity. All gene clusters connected by orthology were grouped together into a single gene cluster family. Chromosomal maps of biosynthetic gene clusters were generated with in-house Python scripts using PySVG (http://codeboje.de/pysvg/).

138 **Results and Discussion**

139 General feature of the *M. ulcerans* Liflandii genome

140 M. ulcerans Liflandii has a 6,399,542 bp genome comprising a single circular 6,208,954 bp 141 chromosome and the previously described 190,588 bp pMUM002 mycolactone megaplasmid, with a 142 G+C content of 65.61% and 62.9% respectively (20). The chromosome is predicted to contain 4,994 143 protein coding DNA sequences (CDS) and 436 pseudogenes (Fig. 1). One rRNA operon and 50 tRNA 144 genes were identified (Table 1). Sequence assembly was complicated by the presence of 231 145 chromosomal copies of the earlier described M. ulcerans insertion sequence IS2404 (208 complete copies) (Fig. 1). The integrity of the finished sequence was verified by reference to a high resolution 146 147 NheI whole-chromosome restriction map (Fig. 2A).

148

Comparisons of the complete chromosomal sequences of *M. marinum* M and *M. ulcerans* Agy99 against *MuL* identified a core genome of 4,237 CDS, which is 85% of total *MuL* coding sequences (Fig. 2B,C). The genetic functional group distribution amongst the three sequenced genomes did not differ significantly across 'intermediary metabolism and respiration', 'cell wall and cell processes', 'conserved hypothetical' or 'lipid metabolism' classes (Fig. 3A). Nucleotide identity amongst the threeway genome comparison of a subset of 3,391 strict core orthologs (excludes paralogs and pseudogenes) was greater than 97% and showed that the highest sequence similarities are between *MuL* and *M*. *marinum* (Fig. 2B). Similarly, the chromosome architecture of *MuL* is more closely related to *M. marinum* M (Fig. 2B), with few genome rearrangements and few large DNA deletions such as those seen in the reduced *M. ulcerans* Agy99 genome. These data are not in contradiction with previous genomic comparisons that indicate a common ancestor for the three lineages of mycolactone-producing mycobacteria, including *MuL* (lineage 1) and *M. ulcerans* Agy99 (lineage 3), and suggest that lineage 3 isolates have undergone accelerated evolution through additional niche adaptation, while *MuL* has retained a more pleomorphic state.

163

<u>JB Accepts published online ahead of print</u>

164 Insertion sequences and phage elements

165 Isolates from all lineages of *M. ulcerans* have more than 200 chromosomal copies of IS2404 (9, 10, 166 21). This element is known to have promoted, at least in part, significant genomic rearrangements in M. ulcerans Agy99, including many large DNA deletions and gene disruptions by insertion (22). The 167 MuL chromosome is 430 kb smaller than M. marinum, but considering that IS2404 sequences 168 169 contribute another 305 kb, it appears that approximately 780 kb has been lost since diverging from a 170 *M. marinum*-like ancestor. Arguably, this difference is largely due to IS2404-mediated deletions. Also, 171 89 of the 224 chromosomal copies of IS2404 (40%) have inserted within CDS. This is comparable to 172 the situation in *M. ulcerans* Agy99, where 97 CDS have been disrupted by IS2404 (45% of the 213 173 copies), although only six copies of IS2404 appear in the same location in both isolates, indicating 174 independent expansion of IS2404 in each lineage. Most startling, however, is that despite the obvious 175 activity of IS2404 in MuL, the 224 copies of this element have had an unexpectedly modest impact on 176 overall chromosome architecture. There are only four major DNA rearrangements in MuL relative to 177 M. marinum M, (all flanked by copies of IS2404), such as a 440 kb inversion between nucleotide 178 positions 2,891,467 and 3,144,394. These four regions are unchanged in *M. ulcerans* Agy99 relative to 179 M. marinum M. The conserved chromosome structure of MuL suggests positive selection for this chromosome arrangement, despite the expansion of IS2404. One conclusion from these observations is that both strains are undergoing independent processes of reductive evolution, where expansion of IS2404 has been equally tolerated but with strong selection for maintenance of chromosome structure in MuL.

184

There are 91 copies of IS2606 in M. ulcerans Agy99 (11, 23). MuL has only 4 copies of IS2606, three 185 186 of which are on pMUM002 (20). The presence of a copy of IS2606 in the same location on both 187 pMUM001 and pMUM002 suggests this IS originated on pMUM and expanded in lineage 3 (20). The 188 single IS2606 (Mlif 03910) chromosomal copy is in stark contrast to the 83 copies in M. ulcerans Agy99 and also highlights the likely role that IS2606 has played in promoting the extensive 189 190 chromosome remodelling seen in the lineage 3 isolates, in particular the preference for IS2606 to insert 191 in close proximity to IS2404. Of the 83 chromosome copies of IS2606, there are 39 instances of IS2606 192 inserting within 100 bp of IS2404 (59 copies within 500bp) and the combination of IS2606 and IS2404 193 are associated with at least 30 instances of inversions and/or deletions (>5000bp) in M. ulcerans 194 Agy99. It is not clear why IS2606 has not similarly expanded in MuL.

195

Two mycobacteriophages, phiMU01 (18 kb) and phiMU02 (24 kb), are variously present in all *M. ulcerans* but not in *M. marinum* M (8). Both phages are present in *MuL*, yet phiMU02 is significantly smaller (13 kb) and phiMU02 CDSs disrupted by IS2606 in *M. ulcerans* Agy99 are mostly deleted or have acquired frameshift mutations in *MuL*.

200

201 M. ulcerans Liflandii regions of difference

To further explore genetic features that might help explain the specific phenotypes of MuL, we examined regions of DNA present only in MuL compared to the other two genomes. In the original 204 description of the *M. ulcerans* Agy99 genome regions of difference (MURDs) were stretches of DNA 205 present in M. marinum M but absent from M. ulcerans Agy99 (11). Here we have defined MuL regions 206 of difference (MULiRD) as regions present only in MuL compared with M. ulcerans and M. marinum. 207 Eleven MULiRDs, spanning 290 CDSs were identified in the genome (Tables S1 & S2). The two 208 largest regions, MULiRD3 (73.9 kb) and MULiRD7 (18.3 kb) (Fig. 1), harbour CDSs with possible 209 roles in secondary metabolism. Both regions are flanked by IS2404 elements and it appears that in M. 210 ulcerans Agy99 these regions were lost by ISE-mediated deletion, where a single copy of IS2404 remains in these locations. MULiRD7 harbours a seven-gene hyc operon (Mlif 03568-Mlif 03574) 211 212 that is duplicated on the chromosome (Mlif 01806 - Mlif 01813), although hycQ (Mlif 01811) is a 213 predicted pseudogene. M. ulcerans Agy99 only has one copy of this operon with the associated 214 transcriptional regulator (MUL 1889) disrupted by a copy of IS2404 and hycE (MUL 1896) containing a 317 amino acid C-terminal truncation. The orthologous hyc locus in M. tuberculosis is 215 thought to encode a formate hydrogenylase complex that is part of a dormancy regulatory network 216 217 involving MprA and DevR, where in *M. tuberculosis* the ortholog of the transcriptional regulator in this 218 locus (Mlif 1806) is upregulated in response to increased concentrations of nitric oxide (24). The 219 preservation and duplication of this system in MuL suggests a similar dormancy response may be 220 important for the lifestyle of the frog pathogen.

221

222 Pseudogene composition of *M. ulcerans* Liflandii

Approximately 8% of all CDSs annotated in *MuL* were predicted to be pseudogenes. Pseudogenes in prokaryote genomes generally occupy 1-5% of all CDSs (25). However, obligate pathogens are thought to be an exception with higher levels of gene inactivation (25). CDSs associated with lipid metabolism (11.5%), cell wall and cell processes (9.3%), and intermediary metabolism-associated proteins (8.0%) were overrepresented with pseudogenes (Fig. 3B). In comparison, *M. ulcerans* Agy99 has 19.8%, 15.5% and 13.4% pseudogenes in the same classes, respectively. The percentage of total coding
sequences in *MuL* that are pseudogenes is intermediate between *M. marinum* and *M. ulcerans* in all
families of proteins (Fig. 3B) with 169 pseudogenes conserved in both *M. ulcerans* Agy99 and *MuL*.

231

Unique to mycobacteria, the cell envelope-associated PE/PPE proteins have been suggested to modulate host immune responses, among other potential functions (26). High DNA identity in the 3' region of these genes is a substrate for recombination and thought to provide a source of antigenic variation among the mycobacteria (27, 28). The highly reduced genome of *M. leprae* contains very few intact CDSs of this family (29). In *M. ulcerans* Agy99, 48.7% of all PE/PPE CDSs are pseudogenes. A significant proportion of these CDSs are also pseudogenes in the *Mu*L genome (28.8%), compared with only 2.2% in *M. marinum* M.

239

240 Mutation and inactivation of certain CDSs (pseudogene formation) in M. ulcerans Agy99 is predicted 241 to have caused some significant phenotypic changes. A frameshift mutation in M. ulcerans Agy99 has 242 resulted in a disruption of cvdA, a component of the cytochrome bd oxidase transporter. However, in 243 MuL cydA is intact. This system is involved in response to anaerobic and hypoxic conditions in vitro in 244 *M. tuberculosis* (30). Conservation of this locus in *MuL* may indicate an increased ability of the frog 245 mycobacterium to survive under low oxygen conditions, although, like M. ulcerans Agy99, the 246 selenocysteine-containing formate dehydrogenase complex, with a predicted role in anaerobiosis, is 247 likely to be inactive in MuL, suggesting it too has an impaired anerobic respiration capacity.

248

Phenolic glycolipids (PGLs) are potent antigens and virulence factors produced by mycobacterial pathogens. PGLs are composed of a polyketide backbone, decorated with species-specific combinations of sugar(s) via a phenolic head group. Genome analysis suggests *Mu*L produces the same PGL as *M. marinum* M, (sometimes called mycoside G). This is distinct to *M. ulcerans* Agy99, where two genes (MUL_1998 and MUL_2001) have been inactivated by mutation resulting in the synthesis of an aglycosylated molecule with a modified polyketide backbone. These two genes are intact in *MuL* (Mlif_1910 and Mlif_1913). The predicted presence of intact PGL in *MuL* might have implications for interactions between host and bacteria and again points to likely differences in the lifestyle of *M. ulcerans* Agy99 compared to *MuL* (11).

258

259 ESX loci

260 Mycobacterial intracellular pathogens such as M. tuberculosis and M. marinum have at least five ESX 261 (or Type VII) ATP-dependent protein secretory systems named ESX-1, 3, 4, 5 & 6. The best defined of 262 these systems, ESX-1, has been implicated in virulence via secretion of certain effectors including the antigens ESAT-6 and CFP-10 (31). MuL has six predicted ESX loci. ESX-1 (6138025 - 6171960) 263 264 appears intact in MuL, although there are two mutations that might impact function. A copy of IS2404 265 has inserted within the intergenic region between the divergently transcribed eccCb1 and the PE35 266 ortholog (Mlif 05720) and this may impact expression of either gene. Also of note, Mlif 05724, the gene immediately downstream of esxA, is a pseudogene, although the M. tuberculosis ortholog 267 (Rv3876) is thought to be non-essential for ESX function (32). ESX-2, immediately downstream of 268 269 ESX-1, shares the same arrangement as in *M. marinum* M and might be inactive, whereas Mlif 05735 270 (the ortholog of MMAR 5460) also appears truncated. The 10 kb region immediately downstream of 271 ESX-2 is disrupted by four copies of IS2404 and thus distinct to M. marinum. ESX-3 272 (218100..230400), ESX-4 (1319227..1332538) and ESX-5 (2592830..2614870) all appear intact, 273 although ESX-5 has a single copy of IS2404 between Mlif 02416 and Mlif 02418. ESX-6 274 (182073..187394) is incomplete with a 7 kb deletion compared to the 12 kb version in M. marinum M, 275 although esxB 2 and esxA 2 in this locus remain intact. In M. marinum M but not in other pathogenic

mycobacteria, the region immediately upstream of ESX-1 contains 11 paralogous predicted membrane proteins of unknown function. This 15.7 kb region is deleted in *MuL*, having been replaced with a single copy of IS2404. This region is also deleted in *M. ulcerans* Agy99. Eleven ESX-1 secretion associated proteins (Esp) are present in *M. marinum* with only four of these proteins intact in the *M. ulcerans* Agy99 genome. *MuL* has mostly conserved these proteins with 10 intact Esp paralogs and one (Mlif_04556) pseudogenized.

282

283 Lipoproteins

284 Lipoproteins in mycobacteria have been implicated in signal transduction (33), evasion of mammalian 285 cells (34) and some have a direct role in virulence as a part of transport systems (35). These proteins 286 can be surface-exposed and anchored by hydrophobic interactions, potentially to mycolic acids within 287 the cell wall (36, 37). Serine proteases like SppA are responsible for hydrolyzing signal peptides prior 288 to export across the cytoplasmic membrane (38). Pre-lipoproteins are then acylated after export from 289 the cytoplasmic membrane by Lgt prior to cleavage by Lsp and Lnt (39). Lipoprotein synthesis appears 290 to be considerably disrupted in MuL as sppA is a pseudogene. In E. coli the sppA homolog specifically 291 cleaves the signal peptide of a major lipoprotein (40). The predicted inability of MuL to cleave N-292 terminal signal peptides from lipoproteins is likely to significantly hamper pre-processing of 293 lipoproteins. The lgt gene is also likely to be inactivated in MuL (8). While not well studied in 294 mycobacteria, prolipoprotein acylation by Lgt is not essential for cleavage by Lsp in different 295 Gram-positive bacteria (41). Despite this, the absence of SppA and Lgt in these M. ulcerans strains 296 may provide a mechanism to reduce the lipoprotein-induced TLR2 response as described in other 297 Gram-positive pathogens (41, 42).

Downloaded from http://jb.asm.org/ on December 12, 2016 by guest

298

300 Genome inspection and metabolic pathway analysis suggests MuL may have some distinctive 301 phenotypic characteristics. Genes encoding DAHP synthases, which are important in the first step of 302 the shikimate enzyme pathway, are pseudogenes. DAHP synthases are responsible for converting 303 erythrose-4-phosphate into 3-deoxy-D-arabino-heptulosonate-7-phosphate during chorismate synthesis 304 (43). Paralogs, aroG (Mlif 02016) and aroG 1 (Mlif 03449) are both disrupted, whilst in M. marinum 305 M there are intact copies of both aroG (MMAR 3222) and aroG 1 (MMAR 1854). In M. ulcerans 306 aroG (MUL 2100) is a pseudogene but aroG 1 (MUL 3533) is intact. Chorismate is an essential 307 precursor for the synthesis of the aromatic amino acids tyrosine, phenylalanine and tryptophan (43) and 308 in *M. tuberculosis*, this pathway is essential for survival (44, 45). The lack of intact *aroG* suggests that 309 MuL may be a tryptophan, tyrosine and phenylalanine auxotroph, and inhabit an environment where 310 these amino acids are available. Experiments to confirm this predicted auxotrophy using Sauton's media supplemented with aromatic amino acids has so far been unsuccessful. 311

312

313 Antibiotic Susceptibility of M. ulcerans Liflandii

In *M. tuberculosis* there is a correlation between isoniazid/ethambutol resistance and the presence of an intact *iniA* gene, as *iniA* is part of an operon proposed to encode an efflux pump involved in resistance to a wide range of antibiotics that target cell wall biosynthesis (46, 47). Upon deletion of *iniA*, *M. tuberculosis* shows increased susceptibility to isoniazid (47). In *Mu*L, all three genes *iniA*, *iniB* and *iniC* are pseudogenes, whereas these genes are intact in both *M. marinum* and *M. ulcerans* Agy99, suggesting other genetic differences in *Mu*L will explain its reported increased resistance to isoniazid and ethambutol compared to *M. ulcerans* Agy99 (2).

321

322 *M. ulcerans* lineage 3 strains are sensitive to rifampicin, which is used in combination with 323 streptomycin to treat Buruli ulcer. In contrast, *MuL* is reported to be resistant to rifampicin (2). Examination of the genome reveals a single amino acid substitution in MuL rpoB (T713M) compared to *M. marinum* and *M. ulcerans*. To our knowledge, the mutation has not been previously reported but it may represent a novel rifampicin resistance mutation. We therefore conducted MIC testing and found MuL 128FXT was fully susceptible to rifampicin (MIC <0.0625 µg/mL), indicating the T713M mutation does not cause rifampicin resistance. The discrepancy with the previous report remains to be explained.

330

331 Secondary metabolism in *M. ulcerans* Liflandii

332 Mycobacteria have diverse secondary metabolite repertoires that include toxins, siderophores and 333 complex cell wall lipids (48). M. marinum M in particular has one of the largest arrays of secondary 334 metabolite gene clusters vet described among bacteria (12), although the metabolites produced by most of these clusters are unknown. We explored the secondary metabolome of MuL using the biosynthetic 335 336 gene cluster search tool antiSMASH (19), and detected 28 distinct secondary biosynthesis clusters on 337 the chromosome. This compares with 33 in M. marinum M, 11 in M. ulcerans Agy99, and 15 in M. 338 tuberculosis F11. To try to compare the secondary biosynthetic potential between these mycobacteria, 339 we classified all 88 antiSMASH-identified gene clusters into 37 families based on their sequence 340 homology (Table S3). MuL has 10 more gene clusters than M. ulcerans Agy99, while the number of 341 pseudogenized gene clusters is similar in both strains (Fig. 4). This analysis reflected the general trend 342 already observed, that lineage 3 M. ulcerans has proceeded further along a reductive evolutionary 343 trajectory than lineages 1 and 2, given that in the genomes of both species numerous gene clusters 344 appear to have been deactivated by pseudogene formation or have been lost by deletion (Fig. 4A).

345

Neither *MuL* nor *M. ulcerans* Agy99 has any gene cluster that is not observed in the *M. marinum* M
genome, and all gene clusters of *M. ulcerans* Agy99 (whether intact or pseudogenized) are also present

348 in MuL (Fig. 4C). This is the expected state for strains that have evolved from a common M. marinum-349 like ancestor. However, there is one intact *M. ulcerans* non-ribosomal peptide synthetase (NRPS) gene 350 cluster that is pseudogenized in MuL (Mlif 01390 - Mlif 01430) and eight intact MuL gene clusters that have been pseudogenized in *M. ulcerans*, indicating that a significant part of reductive biosynthetic 351 352 evolution has taken place independently in both strains and that the products of these loci are not 353 required by the respective specialized bacteria. Mapping the chromosomal positions of the intact and 354 the pseudogene clusters from MuL and M. ulcerans, we observed that gene cluster inactivation has primarily occurred on the leading strand of the right hand replichore, closer to the origin of replication 355 356 than the terminus (Fig. 5). In both MuL and M. ulcerans, seven out of the eight gene clusters, closest to 357 the origin of replication on the leading strand, have been inactivated by pseudogene formation (71% of 358 all pseudogene clusters), even though only two gene clusters are shared in this region between the two 359 genomes. This suggests a general phenomenon and might be explained by the fact that in other 360 bacterial species the same chromosomal region contains the most highly expressed genes (49).

Downloaded from http://jb.asm.org/ on December 12, 2016 by guest

361

362 M. ulcerans ecovar Liflandii

363 There is no consensus on what defines an ecotype, but it has been suggested that an ecotype is a 364 bacterial strain that conserves the genetic potential of a species with genetic differences allowing it to 365 exploit a slightly different ecological niche (50). As discussed previously, MuL fulfils the criteria 366 required for classification within the species M. ulcerans and this is also true for the other 367 mycolactone-producing mycobacteria (9, 10). The comparative genome data we have presented here 368 show that MuL like all M. ulcerans strains is undergoing reductive evolution and is likely also adapting 369 to a niche environment. However, the pattern of mutations, the conserved arrangement of the 370 chromosome and other features such as the distinctive structure and activity of mycolactone E, suggest 371 *MuL* is responding to a different set of environmental pressures compared to *M. ulcerans* Agy99. These

372 lines of evidence lead us to propose that MuL is an ecotype within the species M. ulcerans.

373

374

<u>JB Accepts published online ahead of print</u>

375 Conclusions

376 M. ulcerans Liflandii is a member of the MuMC. The data presented here represent the third complete 377 genome sequence for a mycobacterium from this complex. Like M. ulcerans, the frog mycobacterium 378 has the signature of a niche-adapted organism and contains the pMUM virulence plasmid, several 379 hundred copies of the M. ulcerans-specific insertion sequence IS2404 and many pseudogenes. 380 However, MuL lacks the dramatic DNA rearrangements and deletions seen in M. ulcerans and has a 381 chromosome architecture more closely aligned with M. marinum, MuL shares a large gene repertoire 382 with other members of the MuMC. However, specific mutations in key metabolic pathways such as the 383 aroG/aroG 1 pseudogenes may have a profound impact regarding the environments in which MuL can 384 survive. As with M. marinum, ESX cell wall secretion systems appear to be largely intact in MuL. 385 However, other components of the cell wall are characteristically distinctive, with lipoprotein 386 processing likely to be significantly hampered with non-functional lgt and sppA, dissimilar to both M. 387 ulcerans Agy99 and M. marinum M. We propose that MuL is an ecotype of M. ulcerans, and is 388 adapting to a niche that is related but distinct to other M. ulcerans lineages. The genome sequence of 389 MuL provides an important snapshot of short-term reductive evolution as highlighted by the impact on 390 secondary metabolite biosynthesis gene cluster repertoires. Comparisons with the genomes of M. 391 ulcerans and M. marinum show that such repertoires can change very rapidly, and that they can leave 392 distinct genomic scars, which remain visible for some time and can be uncovered when a closely 393 related genome is available for comparison. Future research could be aimed at better understanding the 394 microbiology (e.g. physiology, biochemistry and antibiotic susceptibility) of M. ulcerans Liflandii, to

try and ascribe the genomic features and predictions made here to confirmed phenotypes for thisunusual pathogen.

397

JB Accepts published online ahead of print

398 Acknowledgements

399 This work was supported in part by grants from the National Health and Medical Research Council of

400 Australia (628640) and the Dutch Technology Foundation STW (STW10463). We are grateful to

401 Rainer Breitling and Eriko Takano for constructive comments that helped improve the manuscript.

JB Accepts published online ahead of print

403	1.	Trott, K. A., B. A. Stacy, B. D. Lifland, H. E. Diggs, R. M. Harland, M. K. Khokha, T. C.
404		Grammer, and J. M. Parker. 2004. Characterization of a Mycobacterium ulcerans-like
405		infection in a colony of African tropical clawed frogs (Xenopus tropicalis). Comp Med 54:309-
406		317.
407	2.	Nigou, J., M. Gilleron, and G. Puzo. 2003. Lipoarabinomannans: from structure to
408		biosynthesis. Biochimie 85:153-166.
409	3.	Fremont-Rahl, J. J., C. Ek, H. R. Williamson, P. L. Small, J. G. Fox, and S. Muthupalani.
410		Mycobacterium liflandii outbreak in a research colony of Xenopus (Silurana) tropicalis frogs.
411		Vet Pathol 48: 856-867.
412	4.	Chai, N., O. Bronchain, G. Panteix, S. Godreuil, C. de Medeiros, R. Saunders, T. Bouts,
413		and A. de Luze. Propagation method of saving valuable strains from a Mycobacterium liflandii
414		infection in Western clawed frogs (Silurana tropicalis). J Zoo Wildl Med 43:15-19.
415	5.	Hong, H., T. Stinear, P. Skelton, J. B. Spencer, and P. F. Leadlay. 2005. Structure
416		elucidation of a novel family of mycolactone toxins from the frog pathogen Mycobacterium sp.
417		MU128FXT by mass spectrometry. Chem Commun (Camb):4306-4308.
418	6.	Mve-Obiang, A., R. E. Lee, E. S. Umstot, K. A. Trott, T. C. Grammer, J. M. Parker, B. S.
419		Ranger, R. Grainger, E. A. Mahrous, and P. L. Small. 2005. A newly discovered
420		mycobacterial pathogen isolated from laboratory colonies of Xenopus species with lethal
421		infections produces a novel form of mycolactone, the Mycobacterium ulcerans macrolide toxin.
422		Infect Immun 73: 3307-3312.

Kaser, M., S. Rondini, M. Naegeli, T. Stinear, F. Portaels, U. Certa, and G. Pluschke.
2007. Evolution of two distinct phylogenetic lineages of the emerging human pathogen *Mycobacterium ulcerans*. BMC Evol Biol 7:177.

- 426 8. Doig, K. D., K. E. Holt, J. A. Fyfe, C. J. Lavender, M. Eddyani, F. Portaels, D. Yeboah 427 Manu, G. Pluschke, T. Seemann, and T. P. Stinear. 2012. On the origin of *Mycobacterium* 428 *ulcerans*, the causative agent of Buruli ulcer. BMC Genomics 13:258.
- Yip, M. J., J. L. Porter, J. A. Fyfe, C. J. Lavender, F. Portaels, M. Rhodes, H. Kator, A.
 Colorni, G. A. Jenkin, and T. Stinear. 2007. Evolution of *Mycobacterium ulcerans* and other
 mycolactone-producing mycobacteria from a common *Mycobacterium marinum* progenitor. J
 Bacteriol 189:2021-2029.
- 433 10. Pidot, S. J., K. Asiedu, M. Kaser, J. A. Fyfe, and T. P. Stinear. 2010. *Mycobacterium*434 *ulcerans* and other mycolactone-producing mycobacteria should be considered a single species.
 435 PLoS Negl Trop Dis 4:e663.
- Stinear, T. P., T. Seemann, S. Pidot, W. Frigui, G. Reysset, T. Garnier, G. Meurice, D.
 Simon, C. Bouchier, L. Ma, M. Tichit, J. L. Porter, J. Ryan, P. D. Johnson, J. K. Davies,
 G. A. Jenkin, P. L. Small, L. M. Jones, F. Tekaia, F. Laval, M. Daffe, J. Parkhill, and S. T.
 Cole. 2007. Reductive evolution and niche adaptation inferred from the genome of *Mycobacterium ulcerans*, the causative agent of Buruli ulcer. Genome Res 17:192-200.
- Stinear, T. P., T. Seemann, P. F. Harrison, G. A. Jenkin, J. K. Davies, P. D. Johnson, Z.
 Abdellah, C. Arrowsmith, T. Chillingworth, C. Churcher, K. Clarke, A. Cronin, P. Davis,
 I. Goodhead, N. Holroyd, K. Jagels, A. Lord, S. Moule, K. Mungall, H. Norbertczak, M.
 A. Quail, E. Rabbinowitsch, D. Walker, B. White, S. Whitehead, P. L. Small, R. Brosch, L.

- Ramakrishnan, M. A. Fischbach, J. Parkhill, and S. T. Cole. 2008. Insights from the
 complete genome sequence of *Mycobacterium marinum* on the evolution of *Mycobacterium tuberculosis*. Genome Res 18:729-741.
- Heysell, S. K., C. Mtabho, S. Mpagama, S. Mwaigwisya, S. Pholwat, N. Ndusilo, J. Gratz,
 R. E. Aarnoutse, G. S. Kibiki, and E. R. Houpt. 2011. Plasma drug activity assay for
 treatment optimization in tuberculosis patients. Antimicrob Agents Chemother 55:5819-5825.
- 451 14. van Hijum, S. A., A. L. Zomer, O. P. Kuipers, and J. Kok. 2005. Projector 2: contig
 452 mapping for efficient gap-closure of prokaryotic genome sequence assemblies. Nucleic Acids
 453 Res 33:W560-566.
- 454 15. Bonfield, J. K., K. Smith, and R. Staden. 1995. A new DNA sequence assembly program.
 455 Nucleic Acids Res 23:4992-4999.
- 456 16. Krzywinski, M., J. Schein, I. Birol, J. Connors, R. Gascoyne, D. Horsman, S. J. Jones, and
 457 M. A. Marra. 2009. Circos: an information aesthetic for comparative genomics. Genome Res
 458 19:1639-1645.
- 459 17. Darling, A. E., B. Mau, and N. T. Perna. 2010. progressiveMauve: multiple genome
 460 alignment with gene gain, loss and rearrangement. PLoS ONE 5:e11147.
- 461 18. Carver, T. J., K. M. Rutherford, M. Berriman, M. A. Rajandream, B. G. Barrell, and J.
 462 Parkhill. 2005. ACT: the Artemis Comparison Tool. Bioinformatics 21:3422-3423.
- 463 19. Medema, M. H., K. Blin, P. Cimermancic, V. de Jager, P. Zakrzewski, M. A. Fischbach, T.
 464 Weber, E. Takano, and R. Breitling. 2011. antiSMASH: rapid identification, annotation and

466		sequences. Nucleic Acids Res 39: W339-346.
467	20.	Pidot, S. J., H. Hong, T. Seemann, J. L. Porter, M. J. Yip, A. Men, M. Johnson, P. Wilson,
468		J. K. Davies, P. F. Leadlay, and T. P. Stinear. 2008. Deciphering the genetic basis for
469		polyketide variation among mycobacteria producing mycolactones. BMC Genomics 9:462.
470	21.	Kaser, M., and G. Pluschke. 2008. Differential gene repertoire in Mycobacterium ulcerans
471		identifies candidate genes for patho-adaptation. PLoS Negl Trop Dis 2:e353.
472	22.	Mahillon, J., and M. Chandler. 1998. Insertion sequences. Microbiol Mol Biol Rev 62:725-
473		774.
474	23.	Stinear, T., B. C. Ross, J. K. Davies, L. Marino, R. M. Robins-Browne, F. Oppedisano, A.
475		Sievers, and P. D. Johnson. 1999. Identification and characterization of IS2404 and IS2606:
476		two distinct repeated sequences for detection of Mycobacterium ulcerans by PCR. J Clin
477		Microbiol 37: 1018-1023.
478	24.	Voskuil, M. I., D. Schnappinger, K. C. Visconti, M. I. Harrell, G. M. Dolganov, D. R.
479		Sherman, and G. K. Schoolnik. 2003. Inhibition of respiration by nitric oxide induces a
480		Mycobacterium tuberculosis dormancy program. The Journal of experimental medicine
		198: 705-713.
481		198:/05-/15.

analysis of secondary metabolite biosynthesis gene clusters in bacterial and fungal genome

Moran, N. A. 2002. Microbial minimalism: genome reduction in bacterial pathogens. Cell 482 25. 483 108:583-586.

465

- Ramakrishnan, L., N. A. Federspiel, and S. Falkow. 2000. Granuloma-specific expression of
 Mycobacterium virulence proteins from the glycine-rich PE-PGRS family. Science 288:1436 1439.
- 487 27. Bottai, D., and R. Brosch. 2009. Mycobacterial PE, PPE and ESX clusters: novel insights into
 488 the secretion of these most unusual protein families. Mol Microbiol 73:325-328.
- 489 28. Delogu, G., and M. J. Brennan. 2001. Comparative immune response to PE and PE_PGRS
 490 antigens of *Mycobacterium tuberculosis*. Infect Immun 69:5606-5611.
- 491 Cole, S. T., K. Eiglmeier, J. Parkhill, K. D. James, N. R. Thomson, P. R. Wheeler, N. 29. 492 Honore, T. Garnier, C. Churcher, D. Harris, K. Mungall, D. Basham, D. Brown, T. 493 Chillingworth, R. Connor, R. M. Davies, K. Devlin, S. Duthoy, T. Feltwell, A. Fraser, N. 494 Hamlin, S. Holroyd, T. Hornsby, K. Jagels, C. Lacroix, J. Maclean, S. Moule, L. Murphy, 495 K. Oliver, M. A. Quail, M. A. Rajandream, K. M. Rutherford, S. Rutter, K. Seeger, S. 496 Simon, M. Simmonds, J. Skelton, R. Squares, S. Squares, K. Stevens, K. Taylor, S. 497 Whitehead, J. R. Woodward, and B. G. Barrell. 2001. Massive gene decay in the leprosy 498 bacillus. Nature 409:1007-1011.

<u>JB Accepts published online ahead of prini</u>

- Shi, L., C. D. Sohaskey, B. D. Kana, S. Dawes, R. J. North, V. Mizrahi, and M. L.
 Gennaro. 2005. Changes in energy metabolism of *Mycobacterium tuberculosis* in mouse lung
 and under in vitro conditions affecting aerobic respiration. Proc Natl Acad Sci U S A
 102:15629-15634.
- Hsu, T., S. M. Hingley-Wilson, B. Chen, M. Chen, A. Z. Dai, P. M. Morin, C. B. Marks, J.
 Padiyar, C. Goulding, M. Gingery, D. Eisenberg, R. G. Russell, S. C. Derrick, F. M.
 Collins, S. L. Morris, C. H. King, and W. R. Jacobs, Jr. 2003. The primary mechanism of

- 23 -

<u>JB Accepts published online ahead of print</u>

506

507

attenuation of bacillus Calmette-Guerin is a loss of secreted lytic function required for invasion of lung interstitial tissue. Proc Natl Acad Sci U S A **100**:12420-12425.

32. Brodin, P., L. Majlessi, L. Marsollier, M. I. de Jonge, D. Bottai, C. Demangel, J. Hinds, O.
Neyrolles, P. D. Butcher, C. Leclerc, S. T. Cole, and R. Brosch. 2006. Dissection of ESAT-6
system 1 of *Mycobacterium tuberculosis* and impact on immunogenicity and virulence. Infect
Immun 74:88-98.

512 33. Steyn, A. J., J. Joseph, and B. R. Bloom. 2003. Interaction of the sensor module of
513 *Mycobacterium tuberculosis* H37Rv KdpD with members of the Lpr family. Mol Microbiol
514 47:1075-1089.

- 515 34. Casali, N., and L. W. Riley. 2007. A phylogenomic analysis of the Actinomycetales *mce*516 operons. BMC Genomics 8:60.
- 517 35. Camacho, L. R., D. Ensergueix, E. Perez, B. Gicquel, and C. Guilhot. 1999. Identification
 518 of a virulence gene cluster of *Mycobacterium tuberculosis* by signature-tagged transposon
 519 mutagenesis. Mol Microbiol 34:257-267.
- 520 36. Kovacs-Simon, A., R. W. Titball, and S. L. Michell. 2011. Lipoproteins of bacterial
 521 pathogens. Infect Immun 79:548-561.
- Wu, C. H., J. J. Tsai-Wu, Y. T. Huang, C. Y. Lin, G. G. Lioua, and F. J. Lee. 1998.
 Identification and subcellular localization of a novel Cu,Zn superoxide dismutase of *Mycobacterium tuberculosis*. FEBS letters 439:192-196.

- Hussain, M., Y. Ozawa, S. Ichihara, and S. Mizushima. 1982. Signal peptide digestion in
 Escherichia coli. Effect of protease inhibitors on hydrolysis of the cleaved signal peptide of the
 major outer-membrane lipoprotein. Eur J Biochem 129:233-239.
- 528 39. Okuda, S., and H. Tokuda. 2011. Lipoprotein sorting in bacteria. Annu Rev Microbiol
 529 65:239-259.
- 530 40. Ichihara, S., N. Beppu, and S. Mizushima. 1984. Protease IV, a cytoplasmic membrane
 531 protein of *Escherichia coli*, has signal peptide peptidase activity. J Biol Chem 259:9853-9857.
- Henneke, P., S. Dramsi, G. Mancuso, K. Chraibi, E. Pellegrini, C. Theilacker, J. Hubner,
 S. Santos-Sierra, G. Teti, D. T. Golenbock, C. Poyart, and P. Trieu-Cuot. 2008.
 Lipoproteins are critical TLR2 activating toxins in group B streptococcal sepsis. J Immunol
 180:6149-6158.
- Machata, S., S. Tchatalbachev, W. Mohamed, L. Jansch, T. Hain, and T. Chakraborty.
 2008. Lipoproteins of *Listeria monocytogenes* are critical for virulence and TLR2-mediated
 immune activation. J Immunol 181:2028-2035.
- 43. Pittard, A. J. 1987. Biosynthesis of the aromatic amino acids., p. 368–394. *In* J. L. Ingraham,
 K. B. Low, B. Magasanik, M. Schaechter, and H. E. Umbarger (ed.), Escherichia coli and
 Salmonella typhimurium : Cellular and Molecular Biology. American Society for
 Microbiology, Washington, DC.
- 543 44. Barker, C., and D. Lewis. 1974. Impaired regulation of aromatic amino acid synthesis in a
 544 mutant resistant to p-fluorophenylalanine. J Gen Microbiol 82:337-343.

- 547 46. Alland, D., A. J. Steyn, T. Weisbrod, K. Aldrich, and W. R. Jacobs, Jr. 2000.
 548 Characterization of the *Mycobacterium tuberculosis iniBAC* promoter, a promoter that responds
 549 to cell wall biosynthesis inhibition. J Bacteriol 182:1802-1811.
- 47. Colangeli, R., D. Helb, S. Sridharan, J. Sun, M. Varma-Basil, M. H. Hazbon, R.
 Harbacheuski, N. J. Megjugorac, W. R. Jacobs, Jr., A. Holzenburg, J. C. Sacchettini, and
 D. Alland. 2005. The *Mycobacterium tuberculosis iniA* gene is essential for activity of an
 efflux pump that confers drug tolerance to both isoniazid and ethambutol. Mol Microbiol
 554 55:1829-1840.
- 555 48. Chopra, T., and R. S. Gokhale. 2009. Polyketide versatility in the biosynthesis of complex
 556 mycobacterial cell wall lipids. Methods Enzymol 459:259-294.
- 49. Rocha, E. P., J. Fralick, G. Vediyappan, A. Danchin, and V. Norris. 2003. A strand-specific
 model for chromosome segregation in bacteria. Mol Microbiol 49:895-903.
- 559 50. Konstantinidis, K. T., and J. M. Tiedje. 2005. Genomic insights that advance the species
 560 definition for prokaryotes. Proc Natl Acad Sci U S A 102:2567-2572.

561

562

563 Tables

564

565 Table 1: Comparison of key genomic features between the three fully assembled genomes of

Feature	M. ulcerans	M. ulcerans	M. marinum	
	Liflandii	Agy99	М	
Chromosome size (bp)	6,208,955	5,631,606	6,636,827	
pMUM plasmid	190,588	174,155	Not present	
G+C content (%)	65.62	65.47	65.73	
Protein CDS	4994	4160	5424	
Unique CDS	268	30	395	
Pseudogenes	436	771	65	
IS2404 copies	239	213	Not present	
IS2606 copies	4	91	Not present	

Downloaded from http://jb.asm.org/ on December 12, 2016 by guest

566 the M. marinum/M. ulcerans complex

567 Figure Legends

568 Fig. 1. Genome map of *M. ulcerans* Liflandii. DNA sequence mapping of the three mycobacterial genomes using M. ulcerans Liflandii as a reference displayed in Circos. The tracks from inside to 569 570 outside represent GC skew, GC content, M. marinum M, M. ulcerans Agy99, ancestral copies of 571 IS2404, all M. ulcerans Liflandii IS2404 copies, pseudogenes present in both mycolactone-572 producing strains but absent in M. marinum M, all M. ulcerans Liflandii pseudogenes, reverse 573 strand CDS, forward strand CDS, assembled M. ulcerans Liflandii genome, major regions of 574 difference MULRD3 and MULRD7. Mapping to pMUM002 is also presented with sequences from 575 M. marinum M excluded from the plot. Sequences for M. ulcerans Agy99 and M. marinum M were 576 obtained from Stinear et al., 2007 and Stinear et al., 2008 (11, 12).

577

Fig. 2. Comparison of *M. ulcerans* Liflandii. A) Alignment of assembled *M. ulcerans* Liflandii chromosome against an NheI optical map. B) ACT Comparison of *M. ulcerans* Agy99 vs *M. ulcerans* Liflandii vs *M. marinum* M vs *M. ulcerans* Agy99. Regions in red indicate identical sequence and orientation and blue indicates identical sequence in the reverse orientation. Indicated are the percentage nucleotide identities among core orthologs. C) Venn Diagram highlighting the number of orthologs between *M. marinum* M, *M. ulcerans* Agy99 and *M. ulcerans* Liflandii.

584

Fig. 3. Functional group distribution. Percentages proportions of **A**) total coding sequences and **B**) pseudogenes by functional group for the sequenced *M. ulcerans/M. marinum* isolates. CDS were classified into one of: intermediary metabolism and respiration (IM & R), cell wall and cell processes (CW & CP), conserved hypotheticals (CH), lipid metabolism (LM), unknown, insertion sequence and phages (IS & P), regulatory proteins (RP), PE/PPE proteins, information pathways (IP) and virulence, detoxification and adaptation (VD & A).

591

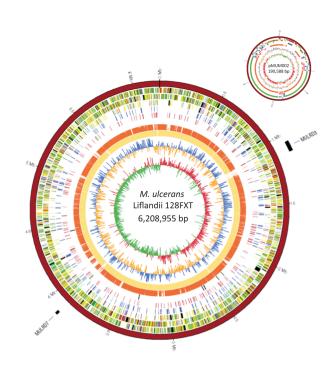
592 Fig. 4. Reductive evolution of secondary metabolite gene clusters in *M. ulcerans* Liflandii. A) 593 Numbers of pseudogene clusters and intact gene clusters in four mycobacterial genomes. Note here 594 that M. marinum and M. tuberculosis may also contain some pseudogene clusters that may have 595 escaped detection due to the lack of a reference strain in which these gene clusters are still intact. B) Phylogram with maximum parsimony-inferred evolutionary events ('+' for gene cluster gain, '-' for 596 597 gene cluster loss and 'P' for pseudogene cluster) in the four mycobacteria, assuming that the 10 598 gene clusters shared by all four mycobacteria represented the ancestral gene cluster repertoire. 599 Probabilities of the three event types were regarded as equal. The numbers behind the species 600 names represent the number of intact and pseudogene clusters in their genomes. Note that reality 601 does not necessarily adhere to maximum parsimony; for example, deletions having occurred in the 602 line towards M. ulcerans may in fact have been preceded by pseudogenes forming before the 603 divergence with M. ulcerans Liflandii. C) Venn diagrams showing which intact and pseudogene 604 clusters are shared between the four mycobacterial genomes.

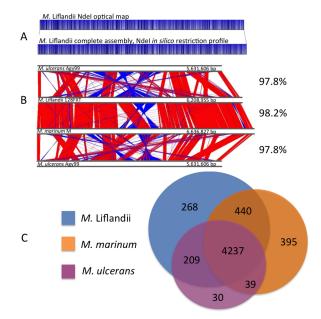
605

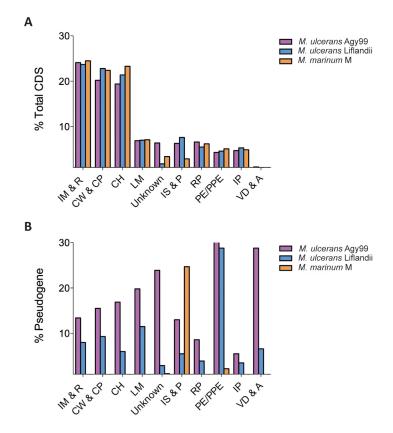
<u>JB Accepts published online ahead of print</u>

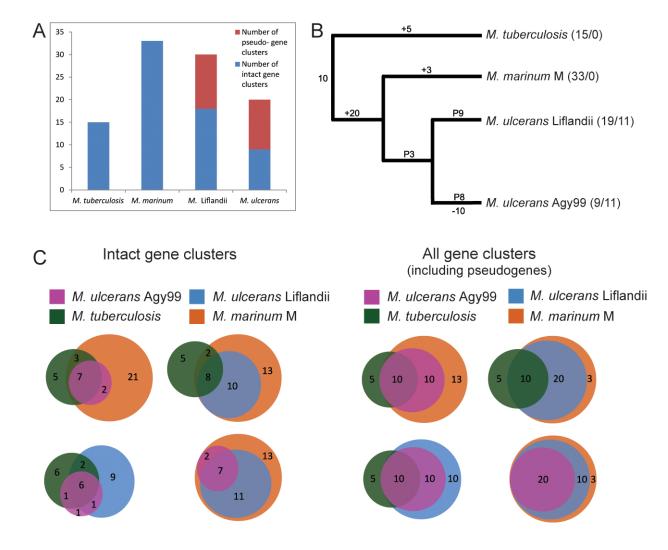
Fig. 5. Inactivation of secondary metabolite gene clusters. The circular chromosomes are displayed in a linearized way, with the origin of replication on the left. Depicted is the predominance of pseudogenes on the leading strand of mycobacterial chromosomes near the origin of replication. Coloured rectangles indicate biosynthetic gene clusters. Colours and connecting lines represent homology between gene clusters in the different genomes. A star marks those clusters that have been inactivated through pseudogene formation.

- 612
- 613
- 614









JB Accepts published online ahead of print

	M. tuberculosis
	M. marinum M
*** ** **	M. ulcerans Agy99